Optical, electrical properties and OH group adsorption of deposits electrolysis

Nabil BOUAZIZI*, Romdhane BEN SLAMA, Bechir CHAOUACHI[1].

Unité de recherché: Catalyse, Environnement et Analyses des Procédés, ENIG, Université de Gabès.

*Corresponding author: Bouazizi Nabil

E-mail : bouazizi.nabil@hotmail.fr

Tel: +216 95 898 970, Fax: +216 75 39 24 21

Abstract:

An electrochemical method, using electrical energy, decompose water into hydrogen and oxygen, which is more important to pH values varying between the intervals {7.9 - 14} and {2-6 - 5}, a degree of salinity lower than 90 g/L and greater than 130 g/L. While the formed film and the resultant powders were characterized by FTIR, UV- Visible and complex impedance. Thus we see that the electrolysis of water causes a change in the stretching vibrations υ_{OH}, namely the presence of Cu-O vibration (solid 520-630 cm^{-1}). A spectral shift in the OH absorption band which is a positive indicator of the interaction of the metal particles dispersed in the electrolyte. Comparison of measurements of the value of pH of the electrolyte showed that acid pH values which increase, which is not the case for basic media and which shows a decrease. A peak of UV-visible absorption at 220 nm was recorded for the solution after production, pH = 8, and two bands at 320 and 360 nm due to hydroxyl compounds that are detected. Furthermore, the complex impedance diagrams show capacitive loops at the high frequency domain, and relaxation process of the electrolyte for different pH values.

Keywords: deposit; salinity; impedance diagrams.

Introduction:

The electrolysis of water is currently only a few percent of the total hydrogen product. And as it is a mode of production own a priori that provides high purity hydrogen. Most exercises prospective energy considering the development of the hydrogen located. Indeed, in transportation applications and under highly stringent climate policies, including hydrogen is widely reported to an important future vector carrier and as the ultimate non-polluting fuel if produced in a sustainable manner [1]. large-scale hydrogen production without consumption of fossil fuels and other emissions, such as gas COx, SOx and NOx is the key to achieving the hydrogen economy [2-3]. Thermochemical cycles [4-5], electrolysis of water [6-7] and photocatalysis process [8-9] are some of the most important fossil processes for producing hydrogen noncombustible. The prospect of higher returns on a massive production of hydrogen excited particular interest to a higher temperature [10].

During this process does not require a high temperature source, in which sunlight, resulting from increasing levels of greenhouse gases in the atmosphere should ensure energy supply, reduce air pollution and meet the growing energy demands of a growing population [11, 12]. Therefore, recent work consider thermal energy sources with lower operating temperatures for the water [13].

The chemical precipitation on the surface of metal, corrodes problem is related to a local solubility. By experience the solubility limit is rarely achieved in all of the liquid, so it is only at a liquid layer on the surface of the metal corrosion product may precipitate. In other words, the product precipitation occurs initially, because the cation diffusion in liquid phase does not dissipate the metal ion flux induced corrosion. The duration of the production has a strong influence on the corrosion and aging of the structure of materials using the repository as controller.

In part to optimize the performance of the electrolysers, the effect of a number of factors must be included, among which are the pH, the temperature, the salinity and the nature of the electrolyte.

The aging of the structure, changes in temperature, voltage dependent on the duration of use, and in our case it is shown that the elevation of temperature due to the kinetics of production, a further increase of the temperature minimizes the flow of hydrogen and the following extension of the duration of use of the arriving material to corrosion.

2. Experimental:

2.1. Hydrogen production:

Currently, the water electrolysis is an electrochemical process, using electrical energy, to decompose water into hydrogen and oxygen (**Fig. 1**), according to two separate chemical reactions taking place at the anode and at the cathode:

$$2H_2O(l) + 2e^- \longrightarrow H_2(g) + 2HO^-$$

-While a hydroxide ion oxidation:

$$2H_2O(l) \longrightarrow O_2(g) + 4H^+(aq) + 4e^-$$

-In both cases, the overall reaction is written as [4]:

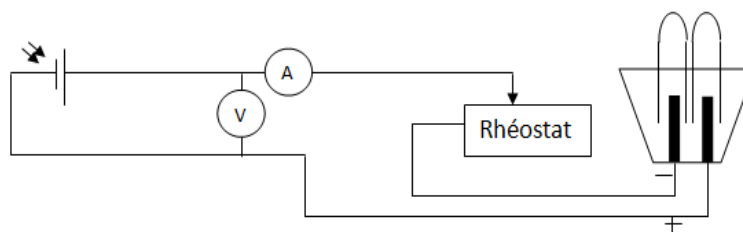$$H_2O(l) \longrightarrow H_2(g) + 1/2\ O_2(g)$$

Fig. 1: Graphic representation of the electrolysis system.

2.2. Synthesis of powder deposition electrolysis

The precipitation of the corrosion of electrolyte material surface changes the local physico-chemical conditions and therefore the continuation of corrosion phenomenon **(Fig. 2)**. The deposit is not a simple diffusion barrier, in fact the corrosion and the deposit a stabilizing solutions are used.

Generally the liquid present in the pores of the deposit, will therefore have a local depletion of diffusing species within the worm liquid surface of the substrate (H $^+$, O_2) and an enrichment of metal species from the ion Al^{3+}.

It is important to have the features of any deposits, after filtration of the latter to give a powder of blue staining.
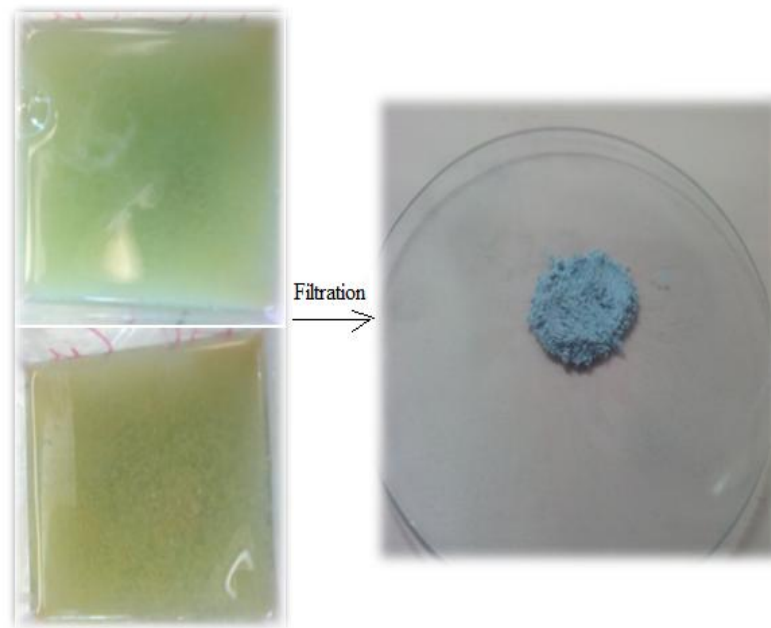
Fig. 2: Deposition observed after hydrogen production and powder obtained after filtration of the film.

2. 3. Characterization:

Infrared Fourier transform spectroscopy to determine the main chemical groups and functions and changes made during their use. Infrared spectra were recorded using a KBr cell Fourier transform IR equipment and infrared spectroscopy (NICOLET IR200). Different methods of implementation allow us to have information on the solution UV-VISIBLE spectrophotometer (SHIMADZU, UV-1650PC). The electrochemical impedance spectroscopy (SIE) is a non-destructive method (Mccafferty, 2010). It allows the identification of the various steps taken in games at an interfacial phenomenon (charge transfer, diffusion corrosion). The electrochemical mounting system for studies in a potentiostat / galvanostat station brand AUTOLAB that can force potential has the working electrode.

A microcomputer equipped with Nova 1.8 software which controls the potentiostat / galvanostat and allows the recording of all electrochemical curves.

3. Results and Discussion:

3.1. Characteristic of the electrolyzer and the photovoltaic panel

The values of current and voltage is recorded and the characteristic curve of the electrolyzer is plotted (**Fig. 3**). The curve of the electrolyser allows us to determine the value of the open circuit voltage to start the electrolysis. This curve varies according to the number of electrolyzer in series, and its surface which can limit the progress of the reaction of hydrogen [20] composition. Thus, the surveys tell us that the trigger voltage electrolysis is V = 18 V.

The curve I_{PV} = f (V_{PV}) reflects its energy behavior under the influence of incident radiation, temperature and load. The experiment is carried out under conditions known as 'natural' as follows: direct sunlight and not in halogen lamp with variable power [3]. For the first steps, the module is fixed in a position and an orientation with an inclination of 35 ° to the horizontal. We choose among the measurements at a maximum variation of solar radiation.

We see **Fig. 4**, the open circuit voltage between 18 V and 20 V. The short-circuiting varies according to sunlight. Sunshine is a much more important parameter the current delivered by the module is proportional to the light received by the module surface.
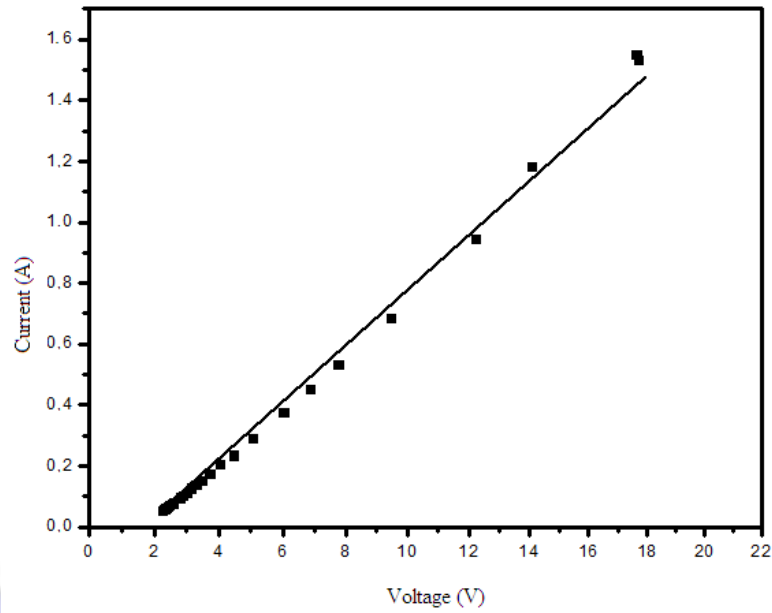
Fig. 3. Change of the intensity of input in the electrolysis according to the voltage
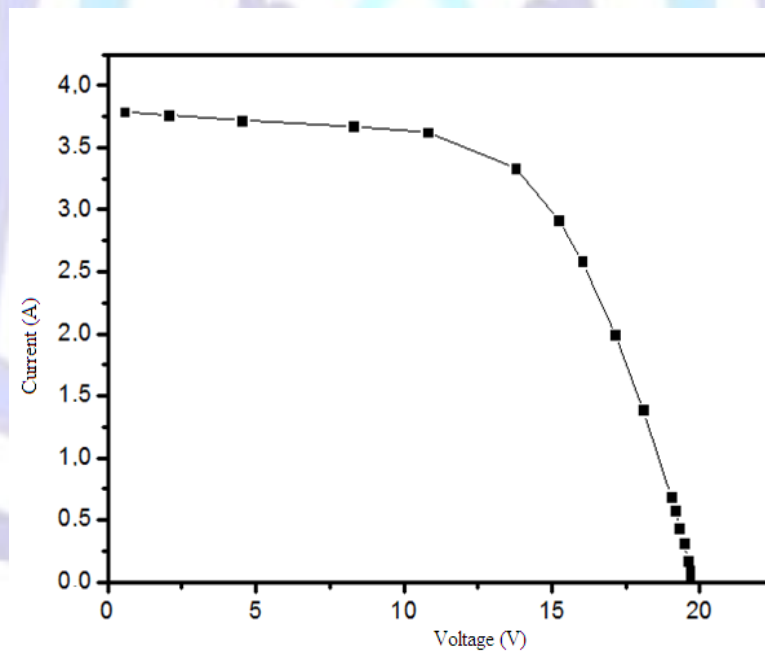

Fig. 4. Characteristics of the photovoltaic module.

3. 2. Mechanism of formation of the deposit

The metal material (aluminum) is in contact with a liquid electrolyte (ions present). The attack is the anode regions [9], and intact to the cathode regions (**Fig. 5)**. Made in the mechanism of corrosion is the following sequence of steps:

(1) Dissociative adsorption water to the substrate surface and formation of hydroxyl groups, (2) migration of the OH of the support surface and the metal transfer, (3) adsorption and dissociation of the water at the surface of metal, (4) desorption of the products.

Also it has been shown that in step (1) is kinetically limited and migration of surface hydroxyl groups of the support.
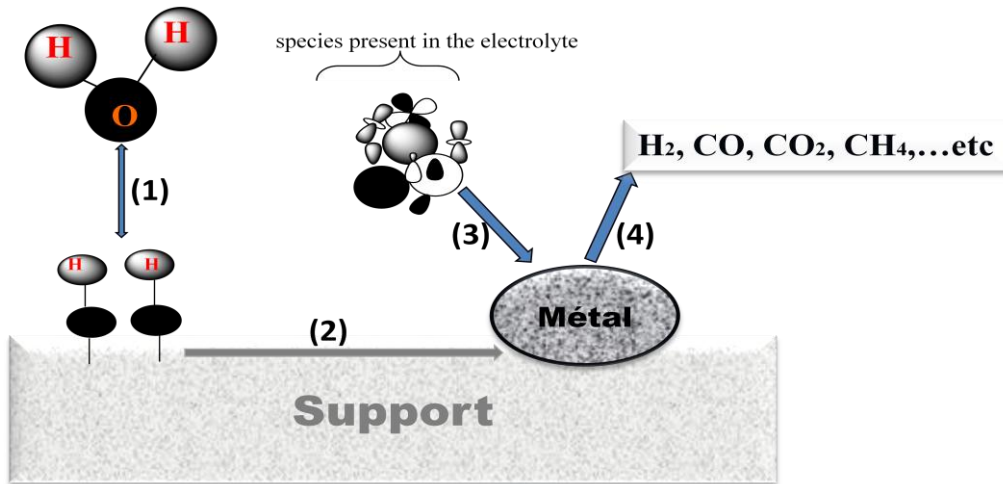
Fig. 5: Schematic representation of the formation mechanism of deposit.

3. 3. Salinity and color variation of the deposit:

The variation of the amount of mass of NaCl affects the coloration of the electrolyte, it is noted that for the masses ranging from 90 to 130 g/L the yellowish coloration persists indicating neutrality of the medium. By cons for less than 90 g/L or greater than 150 g/L masses electrolyte takes the blue color in **(Fig. 6)**.
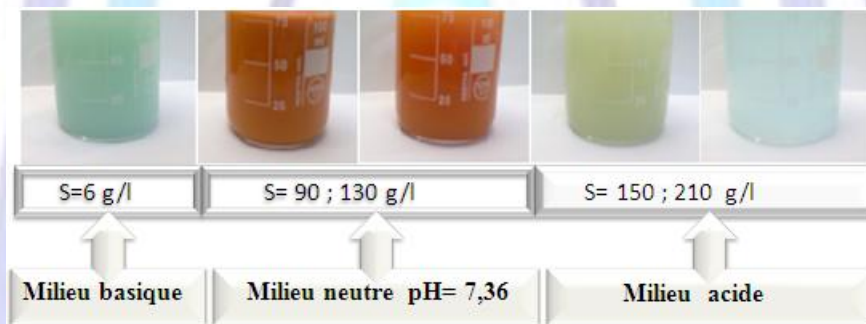

Fig. 6: Change in color of the electrolyte as a function of salinity

(surface electrode S = 17.89 cm^2 in an Electrolyte: tap water, room temperature, atmospheric pressure, voltage U = 19V and h = 3cm).

3. 4. Medium reaction and variation of electric current:

The nature and the phase of the electrolyte which can interfere with the production of hydrogen, while noting changes in the electrolysis system.

To study the influence of pH on the hydrogen flow rate, a series of manipulation has been carried out for different values of pH for the same electrolyte (water discharge valve).

The results shows, that the current density is higher in acid-base environment [8]. While it is lower in neutral media for pH values between 6.4 and 7.4 **(Fig. 7).**
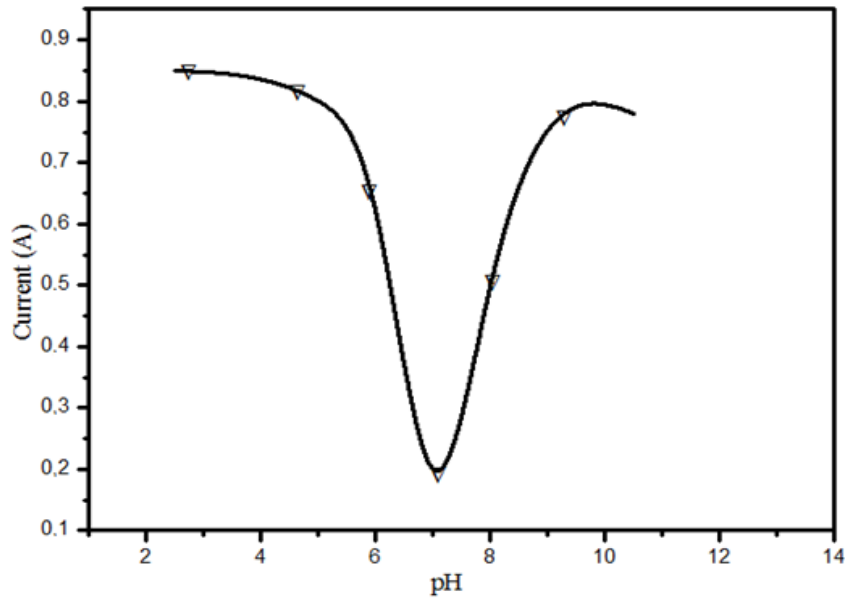
Fig. 7: Dependence of the current I as a function of pH

3. 5. Hydrogen production and pH change

The pH was measured and various carriers are added to the solution at a specified temperature. Aqueous solutions with different initial pH 3.6; 6.3; 8.1; 10 and 12 were prepared and stabilized. Changes in pH values for various solutions before and after hydrogen production are shown in **Fig. 8**. The comparison of measurements of the pH value of the electrolyte showed that acidic pH values increase, which is not the case for the basic media illustrating a decrease. Thus these changes can be explained by the effect of the film caused by the production of hydrogen.
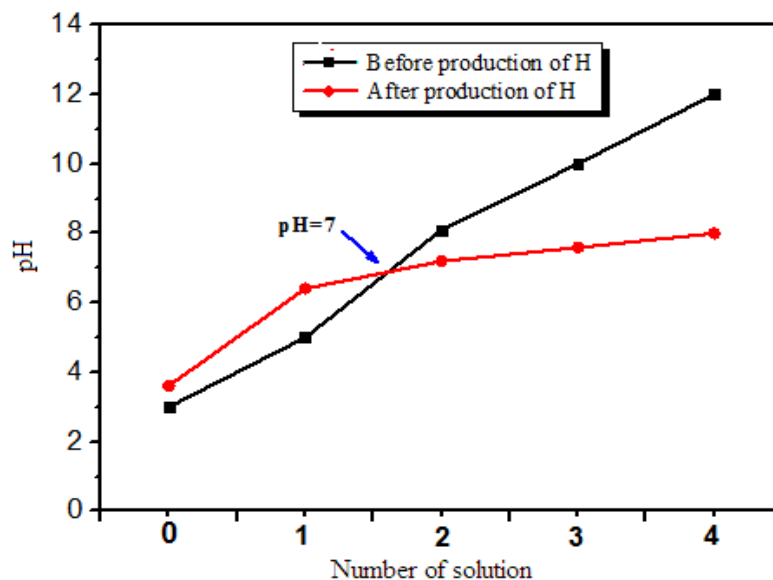

Fig. 8: Variation of the pH versus solution before and after generation of hydrogen.

3. 7. Absorbance of deposit

To identify the species existing in the electrolytic deposition was used the UV-VIS at room temperature. **Fig. 9** shows the UV spectrum of the solution before and after hydrogen production, the only identifiable complex by UV-VIS at room temperature is $AlOH_3$ complex, it has an absorption band at 290 nm attributed to transitions load, which causes a transfer of electrons promotes with a difference of the length of the Al-OH bond. Among other things, this band is assigned to the electronic transition of the resulting hydroxyl group of the strong conjugation between the electrolyte and electrodes.
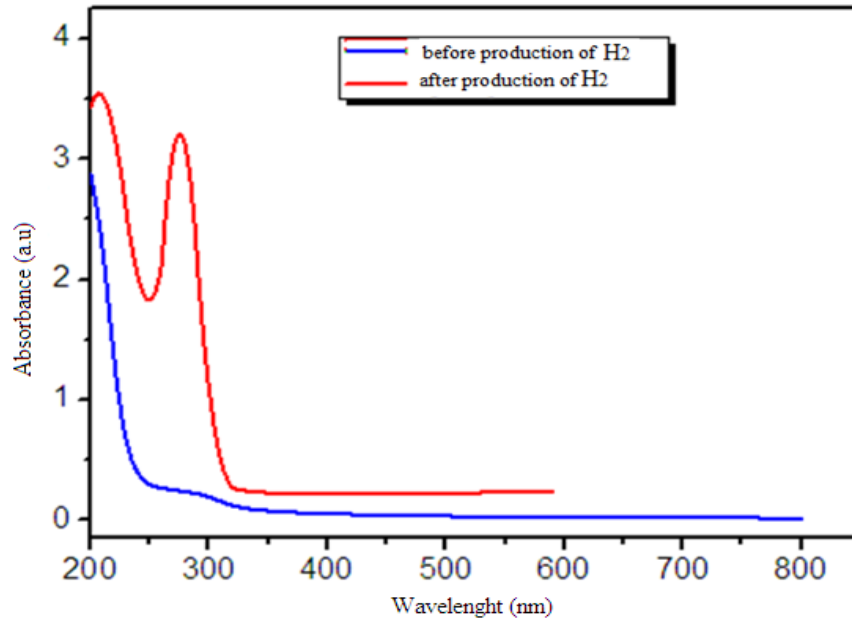
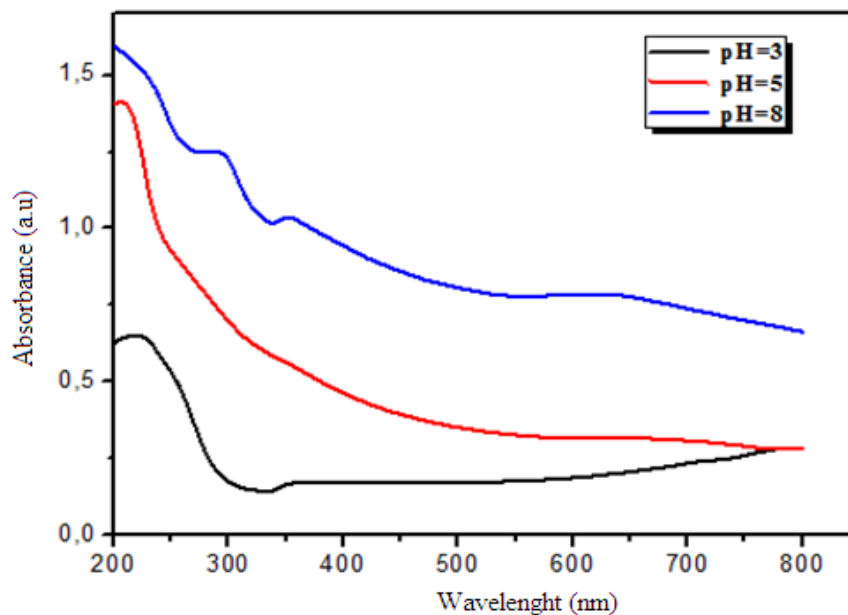**Fig. 9**: UV-VIS spectra of the solution before and after output.

(A surface electrode S = 17.89 cm^2 in an Electrolyte: tap water, room temperature, atmospheric pressure, voltage U = 19V and h = 3cm).

3. 7. 1. Effect of pH:

Fig. 10 is provided, comparative studies of the UV-visible spectra of the electrolyte for different pH values. The absorbance of all the samples having absorption bands around 220 nm, which is more intense to pH = 3, and which moves towards higher energy while increasing the pH value.

This decrease can be explained to the exchange rate existing charges in the electrolyte intensity of the transition is significantly reduced.

At pH = 8, two bands at 320 and 360 nm due to hydroxyl-compounds are detected. The intensity of this band disappeared with the pH decrease to the substitution of Cl ligands by-OH groups-, thereby causing a loss of electrons.

Fig. 10: UV-VIS spectra of the solution for different pH after production.

3. 7. 2. Effect of salinity:

UV spectra recorded at different salinity electrolytes are analyzed, the solutions with mass concentrations of NaCl (6, 50, 110 and 210 g / L) **Fig. 11** were prepared and kept away from light for a week, the time sufficient to balance species is reached. Examination of the results shows the variation of the intensity of the bands detected at 220 nm which are higher for the masses of NaCl: 6 and 210 g / L, and are explained by the development of acid-base game media, while recording the band at 290 nm. However it is gone for other mass concentrations following dependence of the disappearance of species.
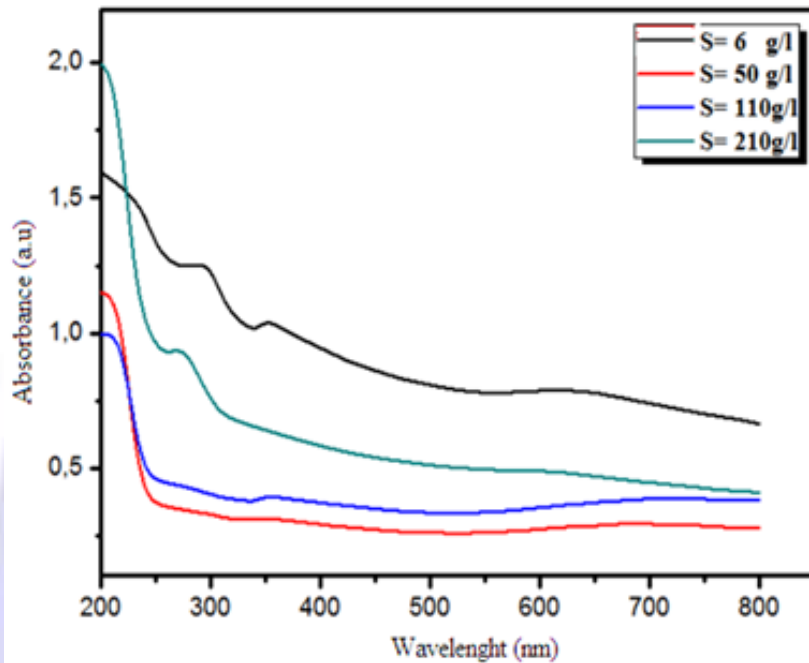

Fig. 11: UV-VIS spectra of the solution for different salinity after production.

## 3.8. Adsorption and electrical properties of the deposit:

3.8. 1. Impedance analysis:

Reactants, products existing in the reaction such as filing, can absorb on the electrode of an electrical point of view, the possibilities of recovery are described by building. Indeed, the diagram is characterized by two capacitive rings which can be attributed to the dispersion of the frequency of the interfacial impedance [21, 22]. The variation of contrast of the imaginary part Z " according to the real part Z ' of the complex impedance stored in tap water (pH = 8.1) to the gypsum and water at ambient temperatures **Fig. 12,** and in a frequency range that extends from (100 kHz - 10 MHz). From these curves, we see that the experimental points are located on arcs passing close to the origin and having centers above the axis real. Therefore, the complex impedance curve of these compounds is represented by the Debye model which suggests the existence of an arc of a circle centered on the real axis. Changing altitudes Z "= f (Z ') for different pH values , and shows the temperature behavior of the thermal resistance of the material. Indeed, any increase is accompanied by a pH decrease of the resistance.
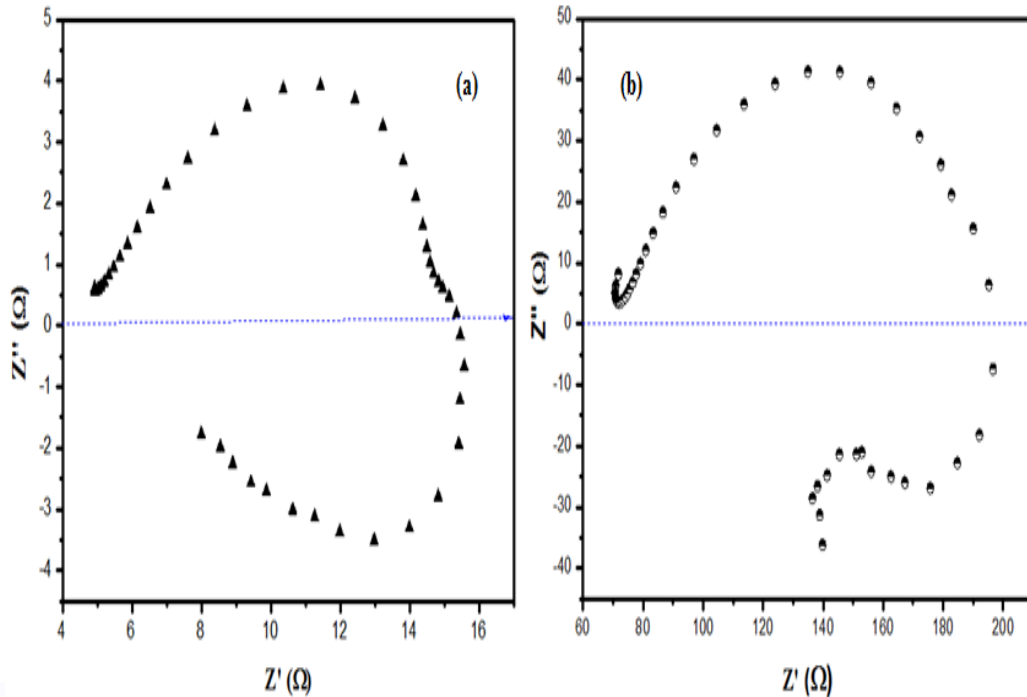
Fig. 12: Complex impedance spectra of compounds: (a) gypsum water (pH = 3.1), (b) tap water (pH = 8.1).

Fig. 13 (a) and **(b)** show, respectively, variations of Z' and Z'' as a function of frequency for different values of pH. Values Z' is quite high in the low frequency region, which is due to the accumulation of free charges at the interface electrode-electrolyte. While for high frequencies, Z' tends towards values close to zero, then that indicates the decrease in the dielectric constant of the material. Furthermore, the Z'' factor has significant values at low frequencies and increases to a pH another, but high frequency curves Z'' show similar behavior at different pH approaching zero.
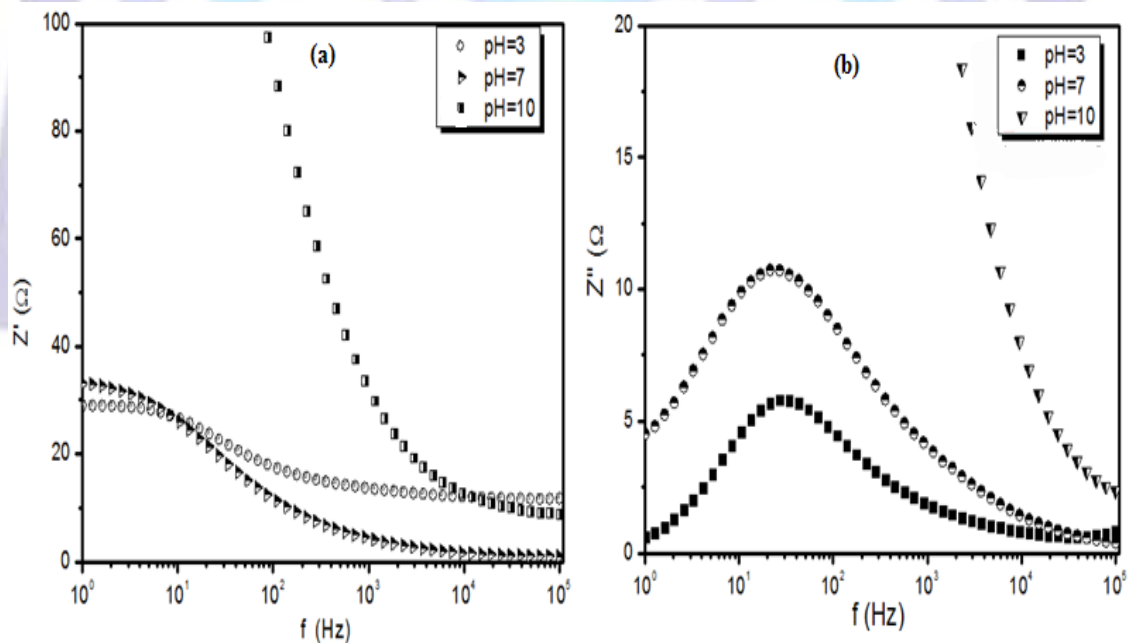
Fig. 13: Variation of real (a) and imaginary (b) parts of impedance as a function of frequency for some representative pH.

The **Fig. 14** (a) ant (b) shows the variation of Z' and Z'' with time, after a minute activity supported on the alumina deposition electrode rapidly increases during the reaction, and then subjected to a free fall Z'' and Z is nearly stable with. This increase can be explained by the electron density at the electrode surface. During the first 75 seconds activate the

electrolyte in the reaction mixture and then disable. Conventionally, the reduction in frequency causes a Z displacement of electrons at ambient temperatures supported on alumina.
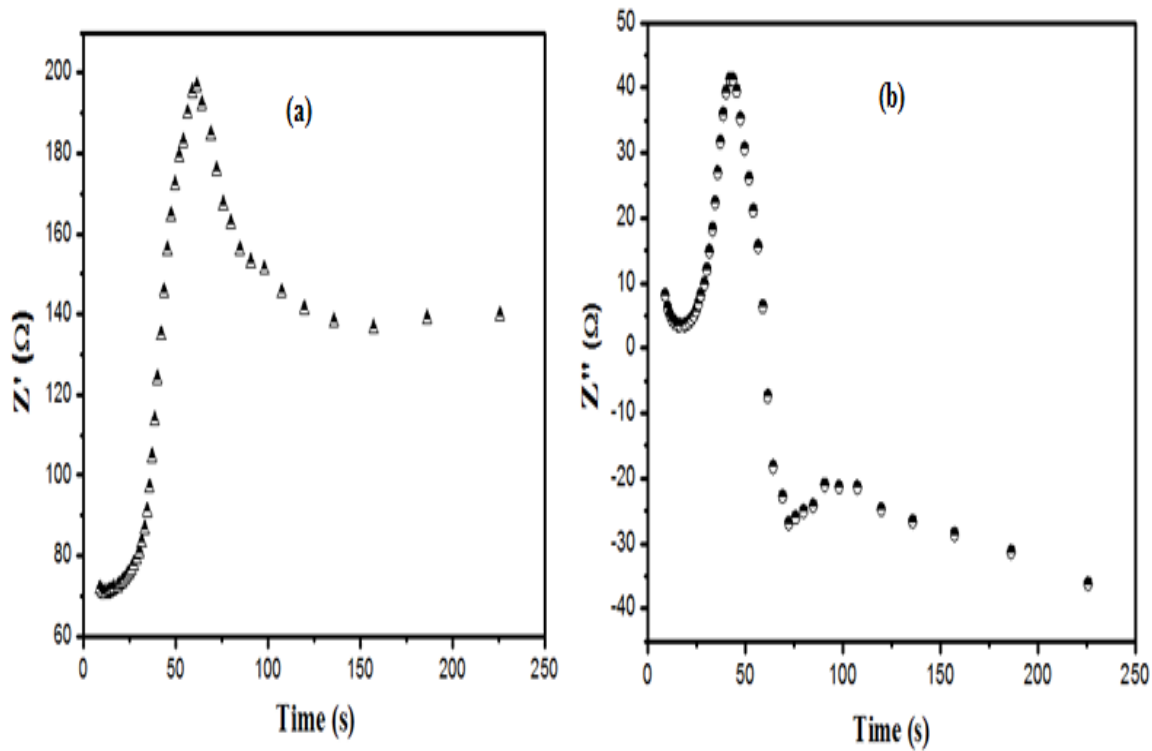

Fig. 14 : dependence of real (a) and imaginary (b) parts of impedance with time.

3.8. 2. Relaxation phenomenon:

Fig. 15 represents the variations of Z' and Z" in the function of frequency at pH = 7. When the frequency increases, Z" increases, while Z' decreases. This trend continues until a particular frequency around which Z" has a maximum value and where it intersects Z'. Moreover, if the frequency continues to increase, Z' and Z" decreases. From 10^3 Hz, both values mingle with the x-axis. This highlights the existence of a relaxation phenomenon. In the other graph shows that the Argand diagram allows determining the resistance as a function of bias and the temperature thereof is dependent on the conductivity [23].
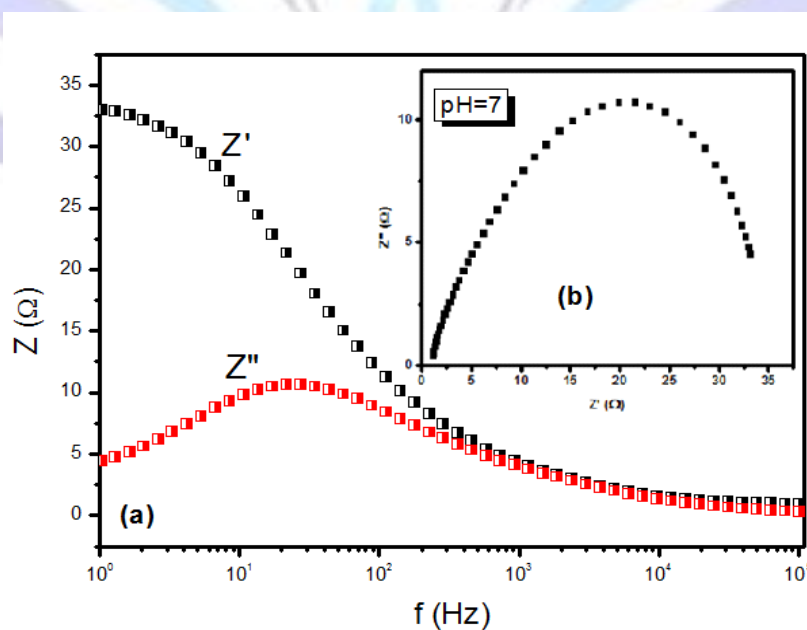

Fig. 15: (a) Argand Diagram (b) Dependence frequency of Z 'and Z ".

The diagrams show a capacitive impedance loop, the high frequency domain, followed by an inductive loop to the field of low frequencies, a capacitive behavior shows the interface in the frequency range examined. The presence of the inductive loop is characterized by the formation of a passivating layer that provides a low frequency negative resistance [24]. The formation of this passivating layer is due to the adsorption. In this case, the interface of an electrode functioning as an electrical circuit with resistors, capacitors inductors [25]. We can therefore try to find an equivalent circuit electrochemical system studied. The electrochemical impedance reflects the contribution of the electrochemical system was observed [26] electrical response. The equivalent circuit is composed of a resistor Re in series with the parallel RC elements **Fig.16.**
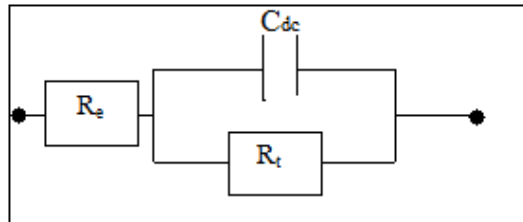
Fig. 16 : Equivalent electrical circuit of the electrolytic deposition.

3.8. 3. Adsorption of OH groups:

Liquid water is a mixture of short and intense hydrogen bonding and long and weak bonds subject to vibration that could cause them to break [12].

The infrared spectrum of hydrogen production electrolyte before (Table.) shows the presence of a wide to 3298 cm^{-1} peak , interpreted to υ_{OH} stretching vibrations , and a peak around 1641 cm^{-1} corresponding to vibration deformation δ_{OH}.

In the case of the electrolyte after production, infrared spectrum associated shows a shift towards the low wavenumber lowest compared to before production, this can be explained by the nature of enter attraction existing chemical species the solution and the OH groups. This spectral difference is a positive indicator of the interaction of the dispersed metal particles with the electrolyte, which provides further evidence providing insights into the strong interactions between hydrogen and oxygen [27]. The electrolysis phenomenon gives rise to an increase of the medium temperature is noted, and leads to the change of the chemical structure. To further improve the characterization of our electrolyte we chose filtration deposit formed while in the comparison with that of the ideal state. Indeed, the examination of the spectra residue is the best way to determine the quality of the analysis results.

The infrared spectra recorded for the samples, electrolyte after use (filing) and the powder are shown.

And reveals the presence of a band at 1600 cm^{-1} corresponding to deformation vibrations δOH for deposit , while this band is largely shifted to wavelengths lower which is in good agreement with the results found Among the above other, a broad absorption band around 3350 cm^{-1} attributable to the stretching vibration υ OH . Noticing a reduction of this band in the case of powder and explained by drying the films in the open area. These results were confirmed showing that produce free OH absorption at 3667 cm^{-1} band [13, 23]. Thus the study by infrared spectroscopy she confirms the presence of hydroxyl species in the film [15, 16, 17, 18].

The strips have the lowest intensity as 600 and 445 cm^{-1} attributed to the stretching vibration of Cu-O are persisted for the powder and which is not the case for the deposit before filtration.

Table. 2: Variation of elongations and deformation vibrations of the OH groups of the electrolyte before and Effective Production of hydrogen,

	deformation δ O-H (cm^{-1})	elongation υ OH (cm^{-1})
Before production of hydrogene	1670.4	3350.8
After production of hydrogene	1636.26	3310.06

Conclusion:

The study of the production of hydrogen by electrolysis of water, and forming the deposition were carried out in this study. Current experimental results are new and important to specify their physicochemical properties. The variation of the mass amount of NaCl affects the color of the electrolyte, but evidence and the nature of the reaction media, including any examination of the results shows that the current density is higher in environments acid-base. In addition, the variation of the pH value before and after production of hydrogen can be explained by the effect of film that changes the yield of hydrogen produced. Different analysis techniques (UV -Vis, IR, and complex impedance spectroscopy) have been used for the characterization of the synthesized powders and films. The UV-visible spectra of the solution before and after the production of hydrogen , which give a single complex may be identifiable to the ambient temperature is $Al(OH)_3$ complex , which presents an absorption band at 290 nm assigned to transitions load , causing promotes transfer of electrons. At pH = 8, two bands at 320 and 360 nm due to hydroxy - compounds are detected. The intensity of this band disappeared with the pH decrease due to the substitution of Cl ligands by OH^- groups. The intensity of the bands detected at 220 nm, which are higher for the masses of NaCl: 210, and 6 g/L, are explained by the development of acid-base game environments.

The study by complex impedance spectroscopy was performed on deposits, this technique allowed the study of the relaxation process of the compound for different pH values. The diagrams show a capacitive impedance loop, the high frequency domain, followed by an inductive loop to the field of low frequencies, a capacitive behavior shows the interface in the frequency range examined. While for high frequencies, Z ' tends towards values close to zero, then that indicates the decrease in the dielectric constant of the material.

A study by infrared spectroscopy shows a redshift in the OH absorption band which is a positive indicator of the interaction of metal particles dispersed with the electrolyte, which provides further evidence providing insights into the powerful interactions from hydrogen and oxygen.

References

[1] Commissioner to Atomic Energy (CEA): review Clefs CEA, new energy technologies, Winter (2005), http://www.cea.fr/.

[2] Sartbaeva. A, Kuznetsov, VL, Wells. SA, Edwards. PP, Energy Environ Sci, 1 (2008) 79-85.

[3] Balthasar. W, Int J Hydrogen Energy, 9 (1984) 649-68.

[4] Kelly. NA, Gibson. TL, Cai. M, Int J Hydrogen Energy, 35 (2010) 892-9.

[5] Onda. K, Kyakuno. T, Hattori. K, Ito. K, J Power Sources, 132 (2004) 64-70.

[6] Wang. M, Wang. Z, Guo. Z, Int J Hydrogen Energy, 35 (2010) 3198-205.

[7] Beghi. GE, Int J Hydrogen Energy, 6 (1981) 555-66.

[8] Gonzales. RB, Law. VJ, Prindle. JC, Int J Hydrogen Energy, 34 (2009) 4179-88.

[9] Ohta. T, 13 (1988) 333-9.

[10] Burgess. G, F-Velasco. JG, Int J Hydrogen Energy 32 (2007) 1225-34.

[11] Kim. J, Van der Bruggen. B, Environ, Pollut, 2 (2010) 335-158.

[12] Ipcc, Ipcc, The Physical Science Basis, (2007).

[13] Rand. D, Dell. R, Hydrogen, RSC publishing (2008).

[14] Rozendal. RA, Hamelers. HVM, Euverink. GJW, Metz. SJ, Buisman. CJN, Int J Hydrogen Energy, 31 (2006) 1632-40.

[15] Martinez. S, Mansfeld-Hukovic. M, J. Appl. Electrochem, 33 (2003) 1137-1142.

[16] Elayyachy. M, El Idrissi. A, Hammouti. B, Corros. Sci,. 48 (2006) 2470-2479.

[17] Long. AR, Adv. Phys, 31 (1982) 553.

[18] Ostermann. E, These de doctorat, Universite Pierre et Marie Curie, (2005).

[19] Franger. S, these de doctorat, Universite Paris, 6 (2001).

[20] Lovedaya. D, Peterson. P, Rodgers. B, JCT Coatings Tech August, (2004) 46-52.

[21] Adrian. S, Claion. R, Spectro-chemical analysis, 18 (2013) 114 – 126.

[22] Aníbal. M, Slavutsky. M, Bertuzzi. A, Margarita. A, María. G, García. N, A. Ochoa, 35 (2013) 270-278.

[23] del Arco. M, Trujillano. R, Rives. V, J, Chem, 8 (1998) 761.

[24] Uzunova. E, Klissurski. D, Mitov. I, Stefanov. P, J, Chem. Mater, 5 (1993) 576.

[25] Hansen. H.C.B, Koch. C.B, Taylor. R.M, J. Solid State Chem, 113 (1994) 46.